$4\times4/8\times8/12\times12$ RECONFIGURABLE MIMO DETECTOR ON MULTI-CORE DSP BASED ON EIGEN DECOMPOSITION OF DATAFLOW GRAPH

†Sheng-Hung Wu, ‡Chien-Yu Kao, ‡Jen-Yuan Hsu, ‡Pang-An Ting, §Gwo-Giun Lee and †Yuan-Hao Huang

†Department of Electrical Engineering and Institute of Communications Engineering,
National Tsing Hua University, Taiwan, R.O.C.
‡Industrial Technology Research Institute, Taiwan, R.O.C.
§Department of Electrical Engineering, National Cheng Kung University, Taiwan, R.O.C.

ABSTRACT

This paper presents a $4\times4/8\times8/12\times12$ and QPSK/16-QAM/64-QAM reconfigurable MIMO detector on a multi-core DSP platform for different MIMO detection algorithms, including multiple-candidate-selection QRSIC (MCS-QRSIC), distributed K-best, and sorting-reduced K-best detectors. This study uses an Eigen-value decomposition method to investigate the intrinsic degree of parallelism of MIMO detectors and allocate the processing elements to DSP cores. MCS-QRSIC outperforms other detectors in 4×4 detection, and distributed K-best has the best performance in 8×8 and 12×12 MIMO systems. The normalized throughput achieves 188/153/142 Mbps for 64-QAM $4\times4/8\times8/12\times12$ MIMO detections at a 1GHz clock rate with 448 cores.

1. INTRODUCTION

Because high-definition multimedia applications are becoming very popular in mobile communication systems, MIMO system has evolved from 4×4 to 8×8 and 12×12 in the next-generation communication systems. ASIC design approach [1–3] sufficiently supports 4×4 and 8×8 MIMO detection. However, the rapid growth of the antenna number leads to difficulties for the design of an MIMO detector on a single chip. Thus, many recent works [4–6] tried to implement the MIMO detector on the multi-core GPU for reconfigurability. However, most of them support only 4×4 MIMO detection and do not explore efficient partition of a MIMO detector on a multi-core platform because of the lower complexity of 4×4 MIMO detector than 8×8 and 12×12 MIMO detectors. Thus, this study presents a platform-independent method [7, 8] to explore the intrinsic degree of parallelism of MIMO detection algorithms. The Eigen-decomposition method can efficiently partition MIMO detection algorithm and allocate operations with the proper number of cores. This study uses a TI TMS320C6678 multi-core DSP processor to analyze the processing cycles and estimate the throughputs under many-core platform. The experiment results show that this design methodology achieves better throughput compared to the available works in the literature.

The rest of this paper is organized as follows. Section II describes the system model and the detection algorithms. Section III introduces Eigen-decomposition method for multi-core MIMO detection algorithms. Section V shows experimental results. Finally, Section VI makes conclusions.

2. MIMO SYSTEM AND DETECTION ALGORITHM

2.1. MIMO System

Assume that an $M \times N$ MIMO system has a flat-fading and uncorrelated channel with additive white Gaussian noise as follows:

$$\tilde{\mathbf{r}} = \tilde{\mathbf{H}}\tilde{\mathbf{s}} + \tilde{\mathbf{n}}, \tag{1}$$

where $\tilde{\mathbf{s}}$ is an $M \times 1$ complex transmitted symbol vector, $\tilde{\mathbf{r}}$ is an $N\times1$ complex received symbol vector, and $\tilde{\mathbf{H}}$ is an $M\times N$ complex channel matrix, which is i.i.d. circular symmetric and every entry of $\tilde{\mathbf{H}}$ is complex Gaussian random variable with 0.5 variance and zero mean per dimension. $\tilde{H}_{i,j}$ represents the channel gain between i-th receive antenna and j-th transmit antenna. $\tilde{\mathbf{n}}$ is a complex Gaussian noise vector. In the DSP implementation, the channel model is reformulated as its equivalent $2M \times 2N$ real channel model.

2.2. MIMO Detection Algorithms

2.2.1. *Multiple-Candidate-Selection QRSIC (MCS-QRSIC)*

MCS-QRSIC [1] aims to address the error propagation problem in the QRSIC detector by selecting C_i candidates for detected symbol $\hat{s}$, as shown in Fig. 1(a). Fig. 1(b) shows the detection path of MCS-QRSIC for 4×4 16-QAM and $(C_4, C_3, C_2, C_1) = (4, 4, 1, 1)$, where four nearest constellation points are selected for $\hat{s}_4$ and $\hat{s}_3$, respectively. Each possible $(\hat{s}_4, \hat{s}_3)$ is used to detect $\hat{s}_2$ and $\hat{s}_1$ by general QR-SIC detection. The corresponding search tree is shown in Figure 1(b). Eventually, there are sixteen detected symbol vectors $(x_{4,i_4}, x_{3,i_3}, x_{2,i_2}, x_{1,i_1})$, where $i_4 = 1, ..., C_4,\ i_3 =$

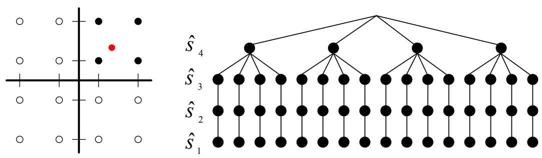

(a) (b)

Fig. 1: (a) Multiple-candidate-selection with $C_i = 4$ and (b) tree expansion for MCS-QRSIC $(4, 4, 1, 1)$.

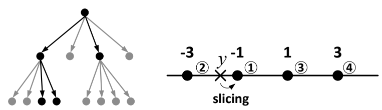

(a) (b)

Fig. 2: (a) Tree expansion for K-best detection (K=2) and (b) Schnor-Euchner enumeration

$1, ..., C_3,\ i_2 = 1, ..., C_2,\ i_1 = 1, ..., C_1$ and $x_{j,i}$ denotes i-th possible symbol for $\hat{s}_j$. We can detect the optimal result from these sixteen paths by the ML detection.

2.2.2. *Distributed K-best Detector*

The generic K-best algorithm fixes the computation complexity in the sphere MIMO detector. However, it usually requires a larger K to achieve an acceptable performance for high-dimensional MIMO and high modulation order. This leads to a large number of partial Euclidean distance (PED) calculations. Thus, distributed K-best detection [2] [9] was proposed to reduce the calculation complexity. The generic K-best detector has to calculate all $K \cdot M$ constellation points for each layer if the modulation size is M (Fig. 2(a)). Therefore, distributed K-best uses Schnor-Euchner enumeration (Fig. 2(b)) to determine the order of the expanded nodes of each parent node. Then, the best nodes are sequentially selected from K best expanded nodes of K parent nodes. This sorting method reduces computation complexity from $(K \cdot M)$ to K for both Euclidean distance and sorting calculations.

2.2.3. *Sorting-Reduced K-best Detector*

The distributed K-best algorithm requires K cycles to search K best child nodes among $K \cdot M$ expanded nodes. The sorting-reduced K-best algorithm aims to further decrease the sorting cycles. Because some child nodes are more likely to be selected, the proposed algorithm directly selects them without sorting. Because the first expanded node of the first parent node has the highest probability, skipping sorting this node can reduce some processing time to some degree without degrading much detection performance. For a (K,S) sorting-reduced K-best, $(K - S)$ specified child nodes are not sorted and S nodes are obtained from sorting. Fig. 3 shows an example for (8,2) sorting-reduced K-best. The specified child nodes are $p = (1, 1, 2, 3, 4, 5)$. The number in p indicates their parent node indices.

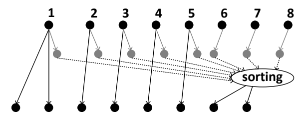

Fig. 3: Signal flow of (8,2) Sorting-Reduced K-best

3. MULTI-CORE ALLOCATION OF MIMO DETECTION ALGORITHMS

This study utilizes an Eigen-decomposition of dataflow graph [7] to evaluate the intrinsic degree of parallism of the MIMO detection algorithms and partition the MIMO detection algorithm on DSP cores accordingly.

3.1. Eigen Decomposition of Dataflow Graph

Given a dataflow graph G of an algorithm composed of n vertexes and m edges. Vertex represents a operation and edge means dependency. The vertex set of G is $V(G) = \{v_1, v_2, ..., v_n\}$ and the edge set of G is $E(G) = \{e_1, e_2, ..., e_m\}$. Then, we can formulate a Laplacian matrix L as follows

$$\mathbf{L}(i,j) = \begin{cases} degree(v_i) & \text{if} \quad i = j \\ -1 & \text{if} \quad v_i \text{ and } v_j \text{ are adjecent} \\ 0 & \text{others} \end{cases} \tag{2}$$

where $degree(v_i)$ is the number of edges connected to the i-th vertex v_i. In the Laplacian matrix, the i-th diagonal entry represents the number of vertexes being connected to v_i and the off-diagonal entry denotes whether two operations are connected.

Let $\mathbf{x}$ be a n variable vector associated with the dataflow graph G. Then, the value of $\mathbf{x^T L x}$ equals to the sum of square differences between adjacent vertexes:

$$\mathbf{x^T L x} = \sum_{(v_i, v_j) \in E(G)} (x_i - x_j)^2, \tag{3}$$

where $(v_i, v_j) \in E(G)$ represents all the operation pairs (v_i, v_j) whose v_i, v_j are linked. $\mathbf{x}$ indicates all the possible ways to cut the graph into two sub-graphs. Then,

$$\mathbf{x^T L x} = 4 \times (\text{size of edge cut}), \tag{4}$$

where size of edge cut is the number of cutted edges.

Now, the next step is to find a partition that minimizes the number of edge cut which could reveal the connectivity of dataflow graph and the intrinsic parallelism. This minimization problem can be formulated as

$$\mathbf{x}^* = arg\ min(\mathbf{x^T L x}) \text{ subject to } \mathbf{x^T x} = 1, \tag{5}$$

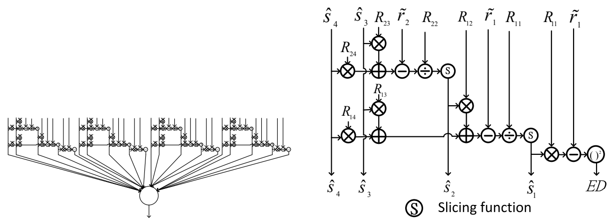

(a) (b)

Fig. 4: (a) Dataflow graph of MCS-QRSIC detector and (b) sub-graph of MCS-QRSIC detector.

By applying Lagrange multiplier, the above constrained optimization problem can be transformed into an unconstrained one. Then, by taking partial derivative with respect to $\mathbf{x}$, the problem becomes an eigen-decomposition equation:

$$\mathbf{L}\mathbf{x} - \lambda\mathbf{x} = 0 \Rightarrow \mathbf{L}\mathbf{x} = 0, \quad (6)$$

The eigenvector with zero eigenvalue becomes the null space of $\mathbf{L}$. Then, the dimension of null space equals the number of zeros, and the degree of parallelism becomes

$$\text{degree of parallelism} = dim(N(\mathbf{L})) = nullity(\mathbf{L}) \quad (7)$$

3.2. Partition of MCS-QRSIC Detector

Fig. 4(a) depicts the dataflow graph of a 2×2 and QPSK MCS-QRSIC detector. The MC-QRSIC detector cannot concurrently search the shortest path and calculate Euclidean distance accross search tree layers due to data dependence between different layers. Thus, we manually cut the graph to create the degree of parallelism. Since Eigen-decomposition method can define either fine-grained operations or coarse-grained operations as vertex. The corresponding Laplacian matrix can then be expressed by

$$Laplacian \quad matrix \ L = \begin{bmatrix} L_A & 0 & 0 & 0 \\ 0 & L_A & 0 & 0 \\ 0 & 0 & L_A & 0 \\ 0 & 0 & 0 & L_A \end{bmatrix}, \quad (8)$$

where L_A represents a 17×17 Laplacian matrix of a coarse-grain set of operations in Figure 4(b). Based on the Eigen-decomposition method (7), the degree of parallelism of MCS-QRSIC detector is four. For a general $N \times N$ M-QAM L-candidate MCS-QRSIC detector, the intrinsic degree of parallelism for cut graph becomes M^{L}.

3.3. Partition of Distributed K-best Detector

K-best decoder cannot also concurrently execute operations among search tree layers. Thus, each tree search layer in distributed K-best must also be executed sequentially. The primary reason is that K best parent nodes must be determined before the next layer performs the accumulated Euclidean distance and sorting calculations. So, we focus on the degree of parallelism in one layer, and Fig. 5(a) shows dataflow graph of a 16-QAM and $K = 3$ distributed K-best detector. One-layer operations (L) are cut into two parts, the accumulation of Euclidean distance and sorting operation. The first part is shown in Fig. 5(b), and its corresponding Laplacian matrix L_A is expressed by Equ. (9). Thus, the Laplacian matrix L is shown in Equation (10). Then, the degree of parallelism is 3. For a general distributed K-best detector, the intrinsic degree of parallelism equals K.

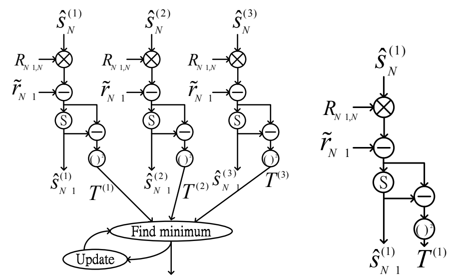

(a) (b)

Fig. 5: (a) Dataflow graph and (b) sub-graph of distributed K-best.

$$Laplacian \quad matrix \ L_A = \begin{bmatrix} 1 & -1 & 0 & 0 & 0 \\ -1 & 3 & -1 & -1 & 0 \\ 0 & -1 & 2 & -1 & 0 \\ 0 & -1 & -1 & 3 & -1 \\ 0 & 0 & 0 & -1 & 1 \end{bmatrix} \quad (9)$$

$$Laplacian \quad matrix \ L = \begin{bmatrix} L_A & 0 & 0 \\ 0 & L_A & 0 \\ 0 & 0 & L_A \end{bmatrix} \quad (10)$$

3.4. Partition of Sorting-Reduced K-best Detector

In the distributed K-best detector, the degree of parallelism of the sorting operations equals 1, and the operations in the following layers cannot be executed in advance due to the data dependence, that is, the K best nodes must be selected to expand nodes for the next layer. Thus, the sorting-reduced K-best detector aims to reduce the sorting latency, and thereby increases the throughput. Its degree of parallelism is the same as that of a distributed K-best detector with the same K.

4. EXPERIMENTAL RESULTS

Figure 6 shows the BER performances of 12×12 MIMO detection for 16-QAM and 64-QAM. For 8x8 and 12x12

Table 1: Comparison with other works

	This work						[4]		[5]		[6]	
Platform	TI TMS320C6678						Nvidia Tesla C2070		Nvidia Tesla C2050		Nvidia 9600GT	
N_{core}	8						448		448		64	
Frequency	1 GHz						1.5 GHz		1.5 GHz		1.625 GHz	
Algorithm	Distributed K-best		Sorting-Reduced K-best		MCS-QRSIC		fully parallel FSD		MMSE		multi-pass trellis traversal	
. Output	Hard		Hard		Hard		Soft		Hard		Soft	
Antenna	4		4		4		4		4		4	
QPSK(Mbps)	0.47	26.43	0.56	31.46	stage=4		212	141	None	None	20.5	88.3
					3.17	177						
16QAM(Mbps)	0.96	53.81	1.06	59.33	stage=2		92.31	61.54	None	None	15.3	65.9
					6.92	387.5						
64QAM(Mbps)	1.325	74.25	1.75	97.88	stage=2		17.2	11.46	70	46	3.8	16.3
					3.37	188						

Table 2: Throughputs for 8×8 and 12×12 MIMO detectors.

	This work					
Platform	TI TMS320C6678					
N_{core}	8					
Frequency	1 GHz					
Algorithm	Distributed K-best		SR K-best		MCS-QRSIC	
. Output	Hard		Hard		Hard	
Antenna	8		8		8	
QPSK(Mbps)	0.44	24.57	0.52	29.1	stage=4	
					3.55	200
16QAM(Mbps)	0.9	50.33	1.01	57	stage=2	
					7.15	400
64QAM(Mbps)	1.272	71.26	1.66	93.3	stage=2	
					2.75	153.77
Antenna	12		12		12	
QPSK(Mbps)	0.41	23.07	0.49	27.31	stage=4	
					1.83	102.62
16QAM(Mbps)	0.85	47.66	0.95	53.17	stage=2	
					3.66	205.2
64QAM(Mbps)	1.27	71.21	1.55	87.1	stage=2	
					2.55	142.77

MIMO detectors, the distributed K-best has the best performance because it efficiently sorts and selects the expanded child nodes in the tree-search detection. Therefore, it can effectively reduce computation complexity. However, K-best algorithm suffers from error floor effect especially for 16-QAM. Fig. 6(a) shows that the MCS-QRSIC outperforms the distributed K-best in BER performance. Fig. 6(a) also shows that the performance of the sorting-reduced 16-QAM K-best approximates that of the distributed K-best K=7 while its cycle count is about 90 % of distributed K-best. For 64-QAM, BER performance of sorting-reduced K-best approaches that of the distributed K-best K=5 while it also saves about 9 % cycle counts. Table 1 compares the proposed MIMO detector with other relative works. The data rates are normalized to 448 cores and 1 GHz clock frequency as follows:

$$\text{normalized data rate} = \frac{(\text{data rate}) \times 448}{\text{frequency} \times \mathrm{N_{core}}} \quad (11)$$

The parameter "stage" for MCS-QRSIC is set 2 or 4 to make the degree of parallelism larger than 16, that is, every core is responsible of at least two paths. MCS-QRSIC has better throughputs for QPSK, 16QAM and 64QAM in 4×4 MIMO detections. In general, the throughput is proportional to the

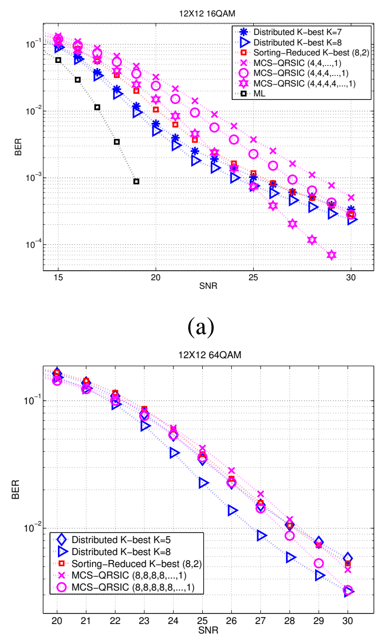

(a)

(b)

Fig. 6: BER Performances of 12×12 MIMO detections for (a) 16QAM and (b) 64QAM.

modulated bits when the MIMO dimension is fixed.

5. CONCLUSION

This paper presents a 4×4/8×8/12×12 configurable MIMO detector on TI TMS320C6678 multi-core DSP processor. An Eigen-decomposition-based method explores the intrinsic degree of parallelism of MIMO detections algorithms and allocates operations to the DSP cores. Because of the efficient allocation of the MIMO detection algorithms, the experiment results shows the better throughput and detection performances compared to the recent works in the literature.

6. REFERENCES

[1] P. L. Chiu and Y. H. Huang, "A scalable MIMO detection architecture with non-sorted multiple-candidate selection," in *Proc. of IEEE International Symposium on Circuits and Systems 2009 (ISCAS 2009)*, May 2009, pp. 689 –692.

[2] M. Shabany and P. Gulak, "Scalable VLSI architecture for K-best lattice decoders," in *IEEE International Symposium on Circuits and Systems 2008(ISCAS 2008)*, May 2008, pp. 940 –943.

[3] Y. Wang and K. Roy, "A new reduced-complexity sphere decoder with true lattice-boundary-awareness for multi-antenna systems," in *IEEE International Symposium on Circuits and Systems 2005(ISCAS 2005)*, May 2005, pp. 4963 – 4966 Vol. 5.

[4] S. Roger, C. Ramiro, A. Gonzalez, V. Almenar, and A. Vidal, "Fully parallel gpu implementation of a fixed-complexity soft-output mimo detector," *IEEE Transactions on Vehicular Technology*, vo. 61 no. 8, p. 3796 – 3800, 2012.

[5] D. Sui, Y. Li, J. Wang, P. Wang, and B. Zhou, "High throughput mimo-ofdm detection with graphics processing units," in *IEEE International Conference on Computer Science and Automation Engineering 2012(CSAE)*, vol. 2, May 2012, pp. 176 –179.

[6] M. Wu, Y. Sun, and J. Cavallaro, "Reconfigurable real-time mimo detector on gpu," in *Conference Record of the Forty-Third Asilomar Conference on Signals, Systems and Computers 2009*, Nov. 2009, pp. 690 –694.

[7] H. Y. Lin and G. G. Lee, "Quantifying intrinsic parallelism via eigen-decomposition of dataflow graphs for algorithm/architecture co-exploration," in *IEEE Workshop on Signal Processing Systems 2010(SIPS)*, Oct. 2010, pp. 317 –322.

[8] G. G. Lee, H. Y. Lin, C. F. Chen, and T. Y. Huang, "Quantifying intrinsic parallelism using linear algebra for algorithm/architecture coexploration," *IEEE Transactions on Parallel and Distributed Systems*, vol. 23, no. 5, pp. 944 –957, may 2012.

[9] S. Mondal, A. Eltawil, C.-A. Shen, and K. Salama, "Design and implementation of a sort-free k-best sphere decoder," *IEEE Transactions on Very Large Scale Integration (VLSI) Systems*, vol. 18, no. 10, pp. 1497 –1501, Oct. 2010.

[10] "[SPRS691B] TMS320C6678 Multicore Fixed and Floating-Point Digital Signal Processor Data Manual," August 2011.